Metabolism Open 15 (2022) 100201

Contents lists available at ScienceDirect

Metabolism Open

journal homepage: www.sciencedirect.com/journal/metabolism-open

Therapeutic effects of aqueous extract of bioactive active component of *Ageratum conyzoides* on the ovarian-uterine and hypophysis-gonadal axis in rat with polycystic ovary syndrome: Histomorphometric evaluation and biochemical assessment

Sunday Aderemi Adelakun [a,*], Victor Okoliko Ukwenya [a], Akwu Bala Peter [b], Adewale Jacob Siyanbade [c], Comfort Oluwakorede Akinwumiju [a]

[a] Department of Human Anatomy, College of Health Sciences, Federal University of Technology, Akure, Nigeria
[b] Department of Anatomy, Kogi State University, Anyigba, Nigeria
[c] Department of Anatomy, Ladoke Akintola University of Technology, Ogbomoso, Nigeria

ARTICLE INFO

Keywords:
Polycystic ovarian syndrome
Ageratum conyzoides
Estradiol valerate
Ovary
Uterus

ABSTRACT

Background: Polycystic ovary syndrome (PCOS) is an endocrine disorder, affecting women of reproductive age. *Ageratum conyzoïdes* (AGC) is used traditionally in the treatment of fever, rheumatism, and ulcer. This study investigates the effects of AGC on ovarian-uterine in PCOS rats.

Methods: Female rats were randomized into four groups (n = 6). Group A control received 2 ml distilled water. Group B received a single dose of 4 mg/kg body weight (bwt) i.p estradiol valerate (EV). Group C received 500 mg/kg bwt AGC and group D received a single dose of 4 mg/kg bwt i.p EV followed by 500 mg/kg bwt AGC orally for 30 days. Parameters tested include follicle-stimulating hormone (FSH), luteinizing hormone (LH), testosterone (T), estradiol (E2), progesterone (P), C-reactive protein (CRP), interleukin (IL)-6, IL-18 and tumor necrosis factor (TNF)- α, malondialdehyde (MDA), superoxide dismutase (SOD), Catalase (CAT), total protein (TP), total cholesterol (TC), triglycerides (TG), low-density lipoprotein cholesterol (LDL), high-density lipoprotein cholesterol (HDL), and ovary and uterus histomorphometric.

Results: Ageratum conyzoides decrease insulin resistance, obesity indices, TC, TG, LDL, MDA, T, LH, FSH, CRP, IL-6, IL-18, and TNF- α in PCOS rats. And increase HDL, E2, P, TP, CAT, and SOD in PCOS rats. AGC improved ovary and uterus histo-architecture, tertiary, and Graafian follicles, corpus luteum and endometrial thickness increased, and cystic and atretic follicles decreased.

Conclusion: Ageratum conyzoides improved insulin sensitivity, antioxidant activities, hormonal imbalance, inflammatory makers, and histological changes in PCOS rats. Therefore AGC can be used as a potential adjuvant agent in the treatment of PCOS.

1. Introduction

Polycystic ovarian syndrome (PCOS) is a gynecological endocrine disorder that affects women of reproductive age [1,2]. Hyperandrogenism is characterized by a hormonal imbalance, chronic menstrual dysfunction (oligo- or anovulation), impaired fertility, hirsutism (excessive body hair growth), acne, obesity, diabetes mellitus, metabolic disturbances (dyslipidemia, hyperinsulinemia, insulin resistance, and type 2 diabetes), increased incidence of endometrial hyperplasia and cancer, and policy [3]. Polycystic ovary syndrome affects around 6–20% of women of reproductive age, and its incidence is on the rise and is the leading cause of female infertility [4,5]. Polycystic ovary syndrome can disrupt ovulation and can lead to infertility; as a result, it is not surprising that infertility affects 70–80% of women with PCOS [6]. In addition, PCOS has been linked to an increased risk of miscarriage, anxiety, and sadness [7]. Also, PCOS is commonly regarded as one of the most significant risk factors for type I endometrial carcinoma (EC) [8]. The primary cause of this elevated risk is thought to be prolonged estrogen exposure to the endometrium as a result of anovulation [9]. As a result, PCOS-related hormonal imbalances can disrupt endometrial tissue homeostasis and stimulate cell growth [10]. Continuous estrogen

* Corresponding author.
E-mail address: anasony2008@gmail.com (S.A. Adelakun).

https://doi.org/10.1016/j.metop.2022.100201
Received 8 June 2022; Received in revised form 16 July 2022; Accepted 16 July 2022
Available online 20 July 2022

Abbreviations

ANOVA	Analysis of variance
ELISA	Enzyme-linked Immunosorbent Assay
EV	Estradiol Valerate
FPG	Fasting plasma glucose
FINS	Fasting insulin
FSH	Follicle-stimulating hormone
GSH-PX	Glutathione peroxidase enzyme
H&E	Hematoxylin and eosin
HOMA-IR	Homeostasis model assessment of insulin resistance
LDL	Low-density lipoprotein cholesterol
LH	Luteinizing hormone
MDA	Malondialdehyde
PCOS	Polycystic ovarian syndrome
SEM	Standard error of the mean
SOD	Superoxide dismutase enzyme

exposure to the endometrium in humans can cause endometrial hyperplasia [11]. Progesterone protects the uterus against estrogen-induced uterine development and proliferation [12]. The primary cause of glucose metabolic disease is insulin resistance (IR), which is also thought to be a key factor in the development of PCOS, which is strongly linked to concurrent metabolic difficulties [3].Low insulin sensitivity, often known as IR, is a syndrome that causes compensatory hyperinsulinemia and plays a significant role in the etiology of type 2 diabetes [4]. Increased levels of testosterone and luteinizing hormone are released as a result of hyperinsulinemia, which disrupts the uptake and utilization of glucose and results in prolonged anovulation [9].Allopathic medications such as clomiphene citrate, metformin, letrozole, tamoxifen, and troglitazone are now the most well-known treatments for PCOS [13]. Hot flushes, arthritis, joint or muscular discomfort, and psychological side effects such as irritability, mood swings, sadness, and bloating are all common adverse effects of allopathic drugs [14]. Since obesity affects the clinical presentation of PCOS, environmental variables including eating habits are crucial in both the prevention and treatment of PCOS. Saturated and trans fatty acid intake will be reduced, and any deficits in vitamins D, chromium, and omega-3 should also be taken into consideration [9]. According to reports, PCOS can result from a lipid-induced proinflammatory state; therefore, a healthy diet with an appropriate macronutrient distribution looks like a suitable choice. The anti-inflammatory properties of the Mediterranean diet (MD) and its link to weight loss make it a suitable dietary treatment for PCOS. Regular consumption of unsaturated fats, low-glycemic carbs, fiber, vitamins, antioxidants, and a modest intake of animal protein is the basis of the MD [9].Alternative therapies such as Laparoscopic ovarian surgery, acupuncture, naturopathy, and herbal medications are gaining popularity as a result of the negative side effects induced by allopathic drugs [15]. The use of plants as traditional medicine has shifted the paradigm away from synthetic drugs and toward natural products (returning to nature) [16,17]. Herbal medical resources are regarded as an important aspect of the natural world [18,19]. Novel active ingredients, particularly those of natural origin, have piqued researchers' curiosity for years due to their unique chemical structures and powerful bioactivities [20,21]. The fact that the majority of therapeutic agents licensed in the previous century were derived from plants or natural sources demonstrates the relevance of plant actives in the creation of innovative medications [22,23]. *Ageratum conyzoides* (AGC) is a medicinal plant that is useful against various ailments such as fever, rheumatism, head arch, colic, burn wounds, dyspepsia, eye problem, uterine disorder, pneumonia, ulcers e.t.c. and may include physiologically active substances that are beneficial to one's well-being [24]. It is an upright, annual herbaceous herb that is native to tropical America, particularly Brazil, and across Africa, save for arid environments [25]. Different tribes in Nigeria have different names for it. The Igedes from the central belt, Yorubas from the southwest, and Igbos from the southeast of the country, for example, refer to it as "ufuopioko," "imiesu," and "nriewu," respectively [26]. The plant grows close to human settlements and thrives in soils rich in nutrients, minerals, and moisture [27]. It can be found in and near waste spaces, gardens, meadows, disturbed habitats, forest borders, watercourses, ruined sites, and other locations, ranging in elevation from sea level to mountainous terrain [28]. Due to its quick growth rates, short life cycles, drought tolerance, allelopathy, increased competitive powers, and higher reproductive capacity, AGC successfully invades natural environments [29]. *Ageratum conyzoides* is a fragrant plant with a long history of use in traditional medicine throughout the world [30]. Several secondary metabolites from AGC have been identified and described, including flavonoids, alkaloids, chromene, terpenoids, coumarins, and sterols, among others [31,32]. Radioactive, antidiabetic, antibacterial, anti-inflammatory, antioxidant, anticancer, and wound healing effects are all claimed for these secondary metabolites [33]. Based on reports of the various beneficial medicinal potential of the bioactive components of AGC, the current study aims to investigate the possible therapeutic and ameliorative effects of aqueous extract of *Ageratum conyzoides* on the ovarian-uterine and hypophysis gonadal axis in a rat with polycystic ovary syndrome.

2. Materials and methods

2.1. Chemical and reagent

Estradiol valerate(NAMAN PHARMA DRUGS, Mumbai.,Mfg.Lic.No.: L/19/2186/MB) was purchased from FEGTOCHI Pharmacy, Akure, Nigeria. Pentobarbital sodium (40 mg/kg, i.p.) was purchased from PASCAL (Nigeria). Thiobarbituric acid and reduced glutathione were purchased from Sigma-Aldrich Corp. (St. Louis, MO USA). Assay kits for protein are products of Randox Laboratories Limited (Co Antrim, United Kingdom) while those of testosterone, follicle-stimulating hormone (FSH), luteinizing hormone (LH), estradiol, progesterone, and leptin were obtained from Monobind Inc. (California, USA). All other reagents used were of analytical grades.

2.2. Plant material and extraction of the plant material

Ageratum conyzoides were harvested in Ondo in October 2021, (Southwest region, Nigeria). A botanist, Mr. Omomoh Bernard, validated the plant at the Herbarium division of the Federal University of Technology Akure, Ondo State Nigeria, where a voucher specimen (FUT/2021/012)was filed for reference purposes. Fresh and clean *Ageratum conyzoides* leaves were air-dried (in the shade), and ground. One kilogram (1 Kg) of the powder was macerated for 12 h in 10 liters of distilled water before being filtered using Whatman paper number 4 [34]. This initial filtrate was kept in the fridge until it was needed. The same amount of distilled water (10 L) was poured into the residue for an additional maceration of 12 h. Following the filtration of this second macerate, the filtrate obtained was added to the first filtrate. The whole was freeze-dried and a total dry mass of 53.53 g of the aqueous extract was obtained. This extract was kept at 4 °C in an airtight container until use [35].

2.3. Phytochemical screening

The aqueous leaf extract of *Ageratum conyzoides* was analyzed qualitatively and quantitatively using a variant of Soni and Sosa's approach [36]. In modifying the study by Grindberg and Williams [37] high-performance liquid chromatography was used to measure the vitamins. The content of minerals such as sodium, calcium, potassium, iron, zinc, and phosphorus was determined using a modified version of the Akubugwo et al. technique [38].

2.4. Experimental animals

In this study, twenty male Sprague Dawley rats (weighing 160–200 g) were employed as experimental animals. At the Animal House of the Department of Human Anatomy, Federal University of Technology, Akure, Nigeria, the rats were kept in plastic cages and kept on a 12:12-h light/dark schedule at room temperature. Rat pellets (Vital Feeds Nigeria Limited, Jos, Nigeria) and unlimited water was given to the rats. The rats were acclimatized for two weeks before treatment and handled humanely following the NIH Guidelines for the Care and Use of Laboratory Animals authorized animal experimental protocols [39].

2.5. Vaginal smears

Each animal's reproductive cycle was determined by collecting vaginal smears daily (8–10 a.m.). Proestrus is characterized by the preponderance of nucleated epithelial cells (the first stage). Cornifield squamous epithelial cells, which appear in clusters, were present during estrus (the second stage). Metestrus (the third stage) is made up of a variety of cell types, with leukocytes predominating with a few nucleated and/or cornifield squamous epithelial cells thrown in for good measure. Diestrus (the fourth stage) is primarily made up of leukocytes [40,41].

2.6. Experimental design

Twenty-four (24) sexually mature female rats were randomized into four groups (A,B,C, and D) of six (n = 6) rats each. Group A served as control and received 2 ml of distilled water. Group B received a single dose (4 mg/kg body weight i.p injection of estradiol valerate (EV) on the first day, Animals in groups C received 500 mg/kg body weight of *Ageratum conyzoides* extract orally, and group D was treated with a single dose (I.P 4 mg/kg body weight) injection of EV on the first day followed by 500 mg/kg body weight of *Ageratum conyzoides* extract orally. All administrations were done once daily for 30 days.

2.7. Assessment of the rat's anthropometric parameters

During the experiment, the rats' initial and end body weight and length were measured daily at roughly 16:00 clocks. To assess obesity in animals, the body mass index (BMI) and the Lee index were determined. By dividing the weight (g) by the length (cm^2), the BMI was computed [43]. The distance between the snout and the anus of rats was used to determine body length. Meanwhile, the Lee index for each animal was calculated by multiplying the complete expression by 1000 and dividing the cube root of the body weight (g) by the naso-anal length (Cm) i.e [LI = body weight $(g)^{1/3}$ x1000/body length (cm)]. If the Lee index score was greater than 310, rats were termed fat [44,45].

2.8. Determination of insulin resistance

The Ultra-Sensitive Rat Insulin ELISA kit (Cloud-Clone Corp., Houston, USA) was used to measure serum insulin concentrations, as reported by Nurdiana et al. [46]. According to Shen et al. [47], the homeostatic model assessment of insulin resistance (HOMA-IR) was calculated as follows:

$$\text{HOMA} - \text{IR}\ (\text{mmol}^{*}\text{mIU/L}^{2}) = \frac{\text{Fasting Blood Glucose (FBG) x Fasting Insulin (FINS)}}{405}$$

2.9. Sample collection

Animals were permitted to fast for 12 h at the end of the trial. The Accu-check Advantage II Blood Glucose Monitor (Roche Mannheim, Germany) was used to measure fasting blood glucose. The highest limit of detection was 33.3 m. After 24 h, animals were sedated with pentobarbital sodium (40 mg/kg, i.p.) [48]. To separate serum, blood samples were taken from the jugular vein and centrifuged for 10 min at 3000 rpm. After then, the samples were kept at −20 °C until they were analyzed. The cervical dislocation was used to slaughter the animals and the ovary and uterine tissues were subsequently separated. After that, the tissues were rinsed with regular saline. One portion of the tissues was preserved in 10% phosphate-buffered formalin for histological investigation [49]. The remaining portion was homogenized in 0.1 M ice-cold Tris-HCl buffer (1/10 w/v, pH 7.4) for biochemical analysis.

2.10. Ovarian homogenate preparation

Using a Potter Elvehjem homogenizer, each rat's left ovary was homogenized individually in 50 mm Tris–HCl buffer (pH 7.4) containing 1.15 percent KCl to generate a 20 percent (1/5 w/v) tissue homogenate. The homogenates were then centrifuged for 10 min at 10,000 g in a chilled centrifuge (4 °C). The supernatants were collected and used to determine total oxidant and antioxidant activity [50].

2.11. Determination of lipid profile

The concentration of the respective parameters; Fasting glucose, triglycerides (TG), total cholesterol (TC), and high-density lipoprotein (HDL) was read directly using a chemistry analyzer (spectrophotometer), whereas the concentration of VLDL was extrapolated by dividing the respective concentration of TG by 5 while LDL-cholesterol estimated using the method by Friedewald et al. [51] that LDL-C = TC -(HDL-C) – Triglycerides/5.

2.12. Determination of serum hormone and inflammatory markers

Enzyme-linked immunosorbent assay (ELISA) kits were used according to the manufacturer's instructions to measure the serum concentrations of hormones [Follicle stimulating hormone (FSH), luteinizing hormone (LH), testosterone (T), estradiol (E2), progesterone (P), inflammatory factors [C-reactive protein (CRP), interleukin (IL)-6, IL-18 and tumor necrosis factor (TNF)- α].

2.13. Determination of ovarian malondialdehyde (MDA)

Ovarian levels of malondialdehyde (MDA) were determined by the method of Wilbur et al. [52]and Adelakun et al. [53]which is based on the reaction with thiobarbituric acid (TBA) at temperature of 90–100 °C. In the TBA test reaction, MDA or MDA-like substances and TBA react with the production of a pink pigment having an absorption maximum at 532 nm. Tissue level of MDA was determined using the following formula: [MDA] = DO/ε.l.m, where [MDA] = concentration of MDA (nM/mg of tissue); DO = absorbance of the sample - absorbance of the reagent blank; ε = molar extinction coefficient (1.56.10–4 nM− 1 cm− 1); l = path length (1 cm); m = mass of the tissue collected for homogenization (mg).

2.14. Determination of ovarian superoxide dismutase (SOD)

Ovarian superoxide dismutase was assayed by the method of Asada et al. [54], which involves the inhibition of photochemical reduction of nitro blue tetrazolium (NBT) at pH 8.0. A single unit of enzyme is defined as the quantity of superoxide dismutase required to produce 50% inhibition of photochemical reduction of NBT. The absorbance was read at 580 nm against a blank using a UV–Vis spectrophotometer. The activity was expressed as U/mg protein.

2.15. Determination of ovarian catalase activity

Catalase activity was estimated by the method of Sinha [55] which is based on the decomposition of H_2O_2 into water. The concentration of undecomposed $H_2O_2$was evaluated using a calibration curve established from a standard solution (50 mM H_2O_2). Tissue catalase activity was determined as follows: C. A = DO/a.t.p, where: C. A = catalase activity (mole of H_2O_2/min/g of total proteins); DO = absorbance of the sample - absorbance of the reagent blank; a = slope of the calibration curve; t = reaction time (1 min); p = ovarian total protein level (g).

2.16. Determination of ovarian total proteins (TP)

Ovarian levels of total peroxidases were determined by the method of Habbu et al. [56] and the method description partly reproduces their wording. Briefly, ovarian homogenate (0.5 ml) was taken, and to this were added 1 ml KI solution (10 mM) and 1 ml sodium acetate (40 mM). The absorbance of potassium iodide was read at 353 nm, which indicates the amount of peroxidase. Then 20 μl of H_2O_2 (15 mM) was added, and the change in the absorbance in 5 min was recorded. Units of peroxidase activity were expressed as the amount of enzyme required to change the optical density by 1 unit per min. The specific activity expressed in terms of units per g of proteins was deduced by the law of Beer-Lambert [57, 58] as follows: C = DO/ε.l.p, where C = concentration of ovarian total peroxidases (mM/g of total proteins); DO = optical density; ε = molar extinction coefficient (11.3 M− 1 cm− 1); l = path length (1 cm); p = ovarian total protein level (g).

2.17. Ovarian and uterine histological procedure

The ovarian and uterine tissues, fixed with 10% formaldehyde were used for histological studies. The tissues were washed overnight in running water to remove the remaining fixative. Dehydration was carried out to remove water using a series of gradually increasing concentrations of alcohol. These tissues were then cleared in xylene embedded in wax and cut in sections of 5-μm thickness using a Rotary Microtome e (micron HM 315 microtome, Walldorf, Germany). The sections were recovered from wax blocks and stained with hematoxylin and eosin (H&E) [59,60]. The sections were viewed and photographed using an Olympus light microscope (Olympus BX51, Tokyo, Japan) with an attached camera (Olympus E−330, Olympus Optical Co. Ltd., Tokyo, Japan).

2.18. Histomorphologicalassessment

Histological analyses of the ovary and the uterus were assessed from 5 μm sections of paraffin-embedded tissues following hematoxylin-eosin staining [61–63]. Histomorphological changes were assessed on microphotographs using a Scientico STM-50 microscope equipped with a Celestron MA411101 camera connected to a computer where the image was transferred and analyzed with the Image J1.3 software. Follicles were recognized and counted in different stages including primary (possess mitotic, cuboidal granulosa cells), preantral (presence of theca and multiple layers of granulosa cells), antral (formed an antrum), Graafian (characterized by a large follicular antrum), cystic (full of liquid) follicles, and corpus luteum. All microscopic measurements for ovary morphometry were done using an eyepiece reticle [64].

2.19. Statistical analysis

Data were analyzed using the GraphPad Prism 8.03 software and are presented as mean ± standard error of the mean (S.E.M.). Statistical significance and the difference among groups were evaluated by one-way analysis of the variance (ANOVA) followed by Tukeys' Post Hoc test for multiple comparisons. Differences were considered significant at $p < 0.05$.

3. Results

3.1. Estrous cycle

Fig. 3 depicts the estrous cycle of control animals, which lasted an average of 5 days and included the following estrous phases: proestrus, estrus, metestrus, and two phases of diestrus. Throughout the research period, rats in the control and AGC alone groups exhibited a consistent estrus cycle of 4–5 days. However, the estrous cycle in PCOS animals was disturbed and halted, and all of the rats' estrus cycles paused following EV injection, generally during the diestrus or metestrus stages. There was cyclic appearance of the various phases of the estrous cycle in animals receiving AGC, beginning with the proestrus phase. The PCOS + AGC therapy group demonstrated better estrous cyclicity. Compared to PCOS rats, there was a higher frequency of the estrus phase and a shorter diestrus phase (see Fig. 2).

Fig. 1. Plant material: *Ageratum conyzoides* Photo: Vijaya Shougrakpam

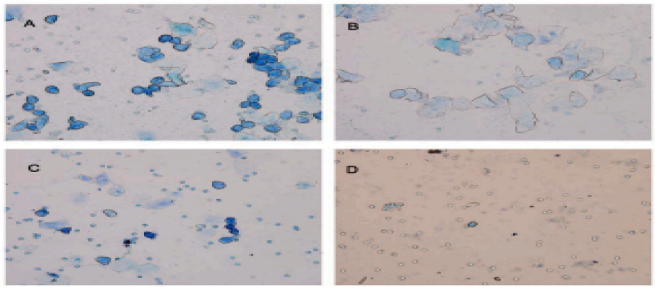

Fig. 2. Vaginal smear figures and cell kinds. Preoestrus contains mostly epithelial cells; estrus contains mostly keratinocytes; metoestrus contains epithelial cells, keratinocytes, and leukocytes; diestrus contains mostly leukocytes (Magnification: ×100) [42].

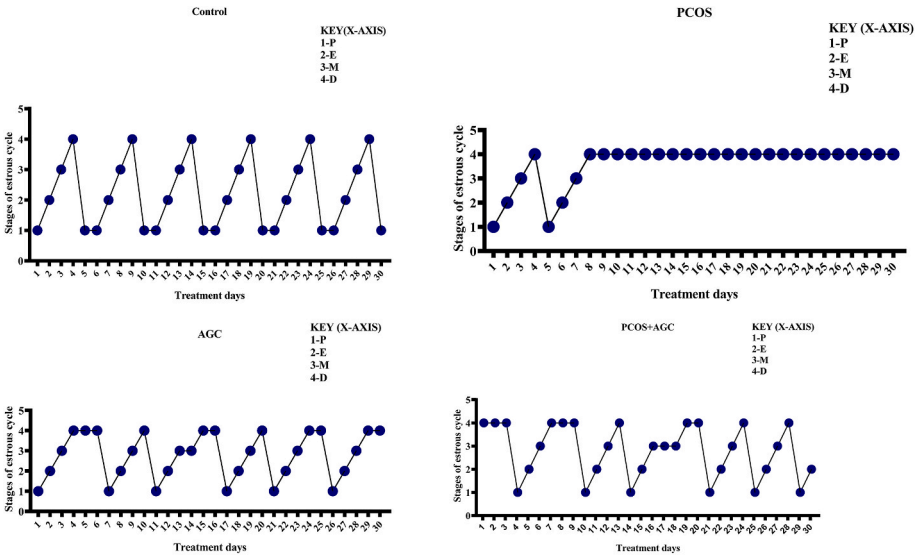

Fig. 3. Effects of *Ageratum conyzoides* extract on estrous cycle in PCOS rats. PCOS: Polycystic ovary syndrome, AGC; *Ageratum conyzoides*. Data show the most represented phase of the estrous cycle in each group, n-6. P = proestrus stage-nucleated epithelial cells, E = estrous stage-cornified cells, M = metestrus-nucleated, cornified and leucocytes, and D = diestrous stage-leucocytes.

Table 1
Qualitative phytochemical analysis of aqueous crude extract of *Ageratum conyzoides*.

S/N	Phytochemicals	status
1	Cardiac glycosides	+
2	Tannins	+
3	Saponins	+
4	Steroids	+
5	Alkaloids	+
6	Flavonoids	+
7	Phenolic acid	+
8	Terpenoids	+
9	Phlobatannins	+
10	Quinones	–
11	Coumarins	–
12	Anthracene	–
13	Sodium	+
14	Potassium	+
15	Calcium	+
16	Phosphorous	+
17	Zinc	–
18	Iron	–

+ Present, – not present.

Table 2
Quantitative phytochemical analysis of aqueous crude extract of Ageratum conyzoides.

S/N	Phytochemicals	Quantity
1	Vitamin A (mg/g)	1.84
2	Vitamin C (mg/g)	1.04
3	Vitamin D (mg/g)	5.54
4	Vitamin E (mg/g)	5.11
6	Total Tannins (%)	6.11
7	Total Saponins (%)	14.32
8	Total Flavonoids (%)	9.75
9	Total Phenols (%)	16.03
10	Total Alkaloids (%)	6.34

3.2. Phytochemical screening

Alkaloids, phlorotannins, flavonoids, tannins, terpenoids, cardiac glycoside, saponins, steroids, sodium, potassium, calcium, and phosphorous were found in Ageratum conyzoides aqueous crude leaves extract [Table 1]. Total saponins, total phenol, and total flavonoids had greater levels after quantitative examination than total tannins and total alkaloids. Vitamins A, C, D, and E were also in great supply [Table 2].

Table 3
Effect of *Ageratum conyzoides* extract on body, ovary, and uterine weight in Polycystic ovarian syndrome rats.

Parameters	Treatment groups			
	Control	PCOS	AGC	PCOS + AGC
Initial body weight (g)	186.80 ± 10.64	188.60 ± 9.78	188.40 ± 7.38	193.20 ± 12.22
Final body weight (g)	208.40 ± 9.41¥	245.20 ± 11.00¥*	214.60 ± 9.91¥α	212.80 ± 10.94¥ α
Weight difference (g)	21.60 ± 1.81	56.60 ± 5.84*	26.20 ± 6.40α	27.60 ± 4.89α
Initial BMI (g/cm2)	0.42 ± 0.02	0.54 ± 0.03*	0.61 ± 0.04	0.59 ± 0.02
Final BMI (g/cm2)	0.46 ± 0.01	0.62 ± 0.02*	0.51 ± 0.02	0.50 ± 0.03
Initial Lee's Index	296.42 ± 4.20	342.60 ± 6.02*	292.82 ± 5.20	310.12 ± 4.22
Final Lee's Index	291.06 ± 4.01	338.22 ± 4.01*	286.32 ± 4.62	298.43 ± 4.46
Abdominal fat weight (g)	2.68 ± 0.18	3.82 ± 0.15*	2.46 ± 0.15α	2.66 ± 0.17 α
Abdominal fat weight (g/100)	1.29 ± 0.11	1.56 ± 0.03	1.16 ± 0.11α	1.26 ± 0.11
Ovary weight (g)	0.26 ± 0.02	0.12 ± 0.01*	0.26 ± 0.01α	0.22 ± 0.03α
Ovary weight (g/100)	0.12 ± 0.01	0.05 ± 0.01*	0.13 ± 0.01α	0.10 ± 0.01α
Uterus weight (g)	0.42 ± 0.03	0.22 ± 0.02*	0.43 ± 0.02α	0.41 ± 0.03α
Uterus weight (g/100)	0.20 ± 0.01	0.09 ± 0.01*	0.20 ± 0.01α	0.19 ± 0.02α

Data presented as mean ± S.E.M, n = 6 in each group, *: represent a significant difference from control, α: represent a significant difference from PCOS at $p < 0.05$, One-Way ANOVA. Follow by Tukey's multiple comparisons test, AGC: *Ageratum conyzoides* PCOS: Polycystic ovary syndrome, BMI: Body mass index.

3.3. Anthropometry parameters of the rats

In all of the experimental groups, there was a marked increase in

final body weight ($p < 0.05$) when compared to beginning body weight. When compared to the control group, the PCOS group's final body and abdominal fat weight increased considerably (p0.05). However, as compared to the PCOS group, the AGC and PCOS + AGC groups showed a substantial reduction in body and abdominal fat weight ($p < 0.05$) [Table 3].

Furthermore, in PCOS-induced rats, there was a significant rise in BMI and Lee index values as compared to controls ($p < 0.05$). During the trial, the mean value of the Lee index was maintained in the PCOS rats. The mean value of the Lee Index in PCOS rats was substantially reduced after treatment with AGC. Meanwhile, in groups treated with AGC and PCOS + AGC, the mean value of BMI and Lee Index decreased significantly ($p < 0.05$) [Table 3].

When compared to the control rats, the PCOS rats had a substantial decrease in ovarian, uterine, and uterine epithelial height ($p < 0.05$). In comparison to PCOS rats, AGC therapy substantially increased ovarian, uterine, and uterine epithelial height ($p < 0.05$). Furthermore, the AGC-treated group only had a significant increase in ovarian, uterine, and uterine epithelial height when compared to the PCOS group ($p < 0.05$), while the AGC-treated group had an insignificant higher value in ovarian, uterine, and uterine epithelial height when compared to the PCOS + AGC treatment group ($p > 0.05$) [Table 3].

3.4. Hormone profile

PCOS causes a substantial increase in testosterone, LH, and FSH levels when compared to the control group ($p < 0.05$). However, as compared to PCOS, post-treatment with AGC lowered the testosterone, LH, and FSH levels ($p < 0.05$). Furthermore, AGC treatment significantly reduced testosterone, LH, and FSH levels when compared to PCOS ($p < 0.05$), and there was no significant difference in testosterone, LH, or FSH between AGC and PCOS + AGC ($p > 0.05$). There was no significant difference in LH/FSH ratio between the control and the experimental groups ($p > 0.05$) [Table 4].

In PCOS, progesterone and estradiol levels were significantly lower than in the control group ($p < 0.05$). In contrast, when compared to PCOS rats, the group treated with AGC and PCOS + AGC exhibited substantial increases in progesterone and estradiol ($p < 0.05$). Between control, AGC, and PCOS + AGC ($p > 0.05$), there was no significant difference in progesterone and estradiol [Table 4].

Table 4
Effect of *Ageratum conyzoides* extract on the hormonal assay of polycystic ovarian syndrome rat.

Parameters	Treatment groups			
	Control	PCOS	AGC	PCOS + AGC
Testosterone (ng/dL)	2.01 ± 0.29	11.86 ± 1.76*	2.29 ± 0.16$^{\alpha}$	3.44 ± 0.48$^{\alpha}$
Luteinizing hormone (IU/L)	5.73 ± 1.53	17.47 ± 3.34*	6.99 ± 1.47$^{\alpha}$	7.45 ± 1.49$^{\alpha}$
Follicle-stimulating hormone (IU/L)	25.09 ± 5.29	79.07 ± 12.79*	22.31 ± 4.96$^{\alpha}$	29.59 ± 6.35$^{\alpha}$
Progesterone (ng/mL)	25.07 ± 4.17	5.48 ± 1.72*	22.66 ± 4.37$^{\alpha}$	21.20 ± 3.92$^{\alpha}$
Estradiol (pg/mL)	13.18 ± 1.65	2.53 ± 0.43*	12.71 ± 1.54 $^{\alpha}$	11.71 ± 1.51 $^{\alpha}$
LH/FSH Radio	0.24 ± 0.06	0.23 ± 0.03	0.36 ± 0.07	0.28 ± 0.05

Data presented as mean ± S.E.M, n = 6 in each group, *: represent a significant difference from control, α: represents significant difference from PCOS at $p < 0.05$, One-Way ANOVA. Follow by Tukey's multiple comparisons test, AGC: *Ageratum conyzoides* PCOS: Polycystic ovary syndrome.

Table 5
Effect of *Ageratum conyzoides* extract on lipid profile in polycystic ovarian syndrome rat.

Parameters	Treatment groups			
	Control	PCOS	AGC	PCOS + AGC
Total cholesterol (mg/dl)	50.23 ± 8.77	85.66 ± 4.79*	45.54 ± 8.46$^{\alpha}$	54.82 ± 8.17$^{\alpha}$
Triglycerides (mg/dl)	50.35 ± 9.64	75.27 ± 10.0*	46.14 ± 9.22$^{\alpha}$	54.13 ± 9.88$^{\alpha}$
HDL-C (mg/dl)	33.15 ± 5.80	17.05 ± 3.14*	36.57 ± 5.97$^{\alpha}$	31.12 ± 5.54$^{\alpha}$
LDL-C (mg/dl)	18.86 ± 3.31	38.71 ± 5.62*	16.90 ± 3.06$^{\alpha}$	21.18 ± 3.68$^{\alpha}$
VLDL-C (mg/dl)	10.07 ± 1.93	15.06 ± 2.00*	9.230 ± 1.84$^{\alpha}$	10.83 ± 1.98$^{\alpha}$
LDL-C/HDL-C	0.58 ± 0.06	1.914 ± 0.39*	0.46 ± 0.05$^{\alpha}$	0.70 ± 0.07$^{\alpha}$
TC/HDL-C	1.73 ± 0.38	5.22 ± 2.15*	1.37 ± 0.29$^{\alpha}$	2.01 ± 0.44$^{\alpha}$
TG/HDL-C	2.44 ± 1.11	5.55 ± 2.68*	1.53 ± 0.49$^{\alpha}$	2.17 ± 0.70$^{\alpha}$

Data presented as mean ± S.E.M, n = 6 in each group, *: represent a significant difference from control, α: represents significant difference from PCOS at $p < 0.05$, One-Way ANOVA. Follow by Tukey's multiple comparisons test, AGC: *Ageratum conyzoides* PCOS: Polycystic ovary syndrome.

3.5. Lipid profile

3.5.1. The cholesterol and triglycerides

In PCOS rats, cholesterol and triglyceride levels were significantly greater ($p < 0.05$) than in the control group. However, as compared to PCOS-induced rats, post-treatment with AGC substantially reduced cholesterol and triglyceride levels ($P < 0.05$). Treatment with AGC reduces cholesterol and triglyceride levels significantly when compared to the PCOS group (<p0.05), but not when compared to the control and PCOS + AGC treatment groups ($p > 0.05$) [Table 5] (see Table 6).

3.5.2. HDL-C, LDL-C, and VLDL

There was observed a significant increase ($P < 0.05$) in LDL-C and VLDL-C in the PCOS group as compared to the control group. But, the level of HDL-C levels reduce significantly in the PCOS group compared to the control ($p < 0.05$). Treatment with AGC after induction of PCOS increased HDL-C and decreased VLDL-C and HDL-C when compared to that of PCOS-induced rats [Table 5].

3.5.3. LDL-C/HDL-C, TC/HDL-C and TG/HDL-C

Also, a significant increase ($P < 0.05$) in ratios of LDL-C/HDL-C, TC/HDL-C, and TG/HDL-C were observed in PCOS rats. However, the

Table 6
Effect of *Ageratum conyzoides* extract on the biochemical assay of polycystic ovarian syndrome rat.

Parameters	Treatment groups			
	Control	PCOS	AGC	PCOS + AGC
Malondialdehyde (nmol/ng protein)	2.03 ± 0.30	9.01 ± 1.26*	1.91 ± 0.28$^{\alpha}$	2.49 ± 0.46$^{\alpha}$
Superoxide dismutase (μmole/g total proteins)	12.18 ± 2.21	3.79 ± 0.86*	9.92 ± 2.02$^{\alpha}$	14.41 ± 2.09$^{\alpha}$
CAT (U/mg protein)	25.91 ± 5.87	6.08 ± 1.58*	23.08 ± 5.52$^{\alpha}$	23.77 ± 5.62$^{\alpha}$
Total peroxidases (mM/g of total proteins)	31.12 ± 3.08	11.07 ± 2.35*	28.63 ± 3.23$^{\alpha}$	27.90 ± 2.38$^{\alpha}$

Data presented as mean ± S.E.M, n = 6 in each group, *: represent a significant difference from control, α: represents significant different from PCOS at $p < 0.05$, One-Way ANOVA. Follow by Tukey's multiple comparisons test, AGC: *Ageratum conyzoides* PCOS: Polycystic ovary syndrome.

intervention of AGC significantly reduced the mean value of ratios of LDL-C/HDL-C, TC/HDL-C, and TG/HDL-C compared to that of the PCOS group. No significant difference in ratios of LDL-C/HDL-C, TC/HDL-C, and TG/HDL-C mean value of control, AGC, and PCOS + AGC treatment groups ($p > 0.05$) [Table 5].

3.6. Ovarian oxidant and antioxidant parameters

The ovarian MDA levels of PCOS animals were significantly higher relative to the control ($p < 0.05$). Compared to the PCOS group, the mean value of ovarian MDA in the AGC and PCOS + AGC therapy groups decreased significantly ($p < 0.5$). In addition, the PCOS + AGC group had a somewhat higher value than the control and AGC groups ($p > 0.05$).

In comparison to the control group, the concentrations of SOD, CAT, and TP in the ovary decreased significantly ($p < 0.05$). Relative to the PCOS group, therapy with just AGC and after treatment with AGC significantly increased ovarian SOD, CAT, and TP concentrations ($p < 0.05$). [Fig. 6].

3.7. Serum inflammatory markers

There was an observed significant increase in serum TNF-α, CRP, IL-6, and IL-18 in PCOS rats in comparison to control ($p < 0.05$). The administration of AGC alone and post-administration of AGC after PCOS induction significantly reduced the level of TNF-α, CRP, IL-6, and IL-18 relative to the PCOS group ($p < 0.05$). When compared to the control, AGC, and PCOS + AGC groups recorded no significant difference in TNF-α, CRP, IL-6, and IL-18 ($p > 0.05$).However, AGC presents an insignificant lower value in TNF-α, CRP, IL-6, and IL-18 than the control and PCOS + AGC ($p > 0.05$) [Table 7].

3.8. FBG, FINS, and HOMA-IR

Data on fasting blood glucose (FBG), fasting insulin (FINS), and HOMA-IR results are displayed in Fig. 4. FBG, FINS, and HOMA-IR levels were significantly increased in PCOS rats than in the control group ($p < 0.05$). In contrast to the PCOS group, rats in the AGC and PCOS + AGC therapy groups had significantly decreased FBG, FINS, and HOMA-IR values (<p0.05). FBG, FINS, and HOMA-IR values did not change significantly between the control, AGC, and PCOS + AGC therapy groups ($p > 0.05$) [Fig. 4].

3.9. Number of primary, secondary, and tertiary follicles

When comparing the PCOS group to the control group, the number of primary, secondary, and tertiary follicles decreased significantly ($p < 0.05$). In comparison to the PCOS group, post-administration of AGC following PCOS induction reversed this impact by substantially increasing the number of primary, secondary, and tertiary follicles ($p < 0.05$). In addition, as compared to the control, the number of primary follicles increased significantly in the AGS and PCOS + AGC therapy groups ($p < 0.05$). Between the AGC and PCOS + AGC experimental groups, no significant differences in primary, secondary, or tertiary follicles were recorded ($p > 0.05$) [Fig. 5].

Table 7
Effect of *Ageratum conyzoides* extract on inflammatory markers of polycystic ovarian syndrome rat.

Parameters	Treatment groups			
	Control	PCOS	AGC	PCOS + AGC
TNF-α (ng/g protein)	19.13 ± 4.94	48.01 ± 9.08*	16.31 ± 4.69$^{\alpha}$	23.09 ± 5.41$^{\alpha}$
CRP (ng/g protein)	19.53 ± 6.48	56.84 ± 13.62*	17.51 ± 6.01$^{\alpha}$	22.07 ± 6.82$^{\alpha}$
IL-6 (ng/g protein)	26.25 ± 8.66	60.40 ± 17.26*	23.50 ± 8.24 $^{\alpha}$	27.74 ± 8.79$^{\alpha}$
IL-18 (ng/g protein)	4.52 ± 1.61	15.33 ± 3.32*	3.73 ± 1.24$^{\alpha}$	5.85 ± 1.59$^{\alpha}$

Data presented as mean ± S.E.M, n = 6 in each group, *: represent a significant difference from control, α: represent a significant difference from PCOS at $p < 0.05$, One-Way ANOVA. Follow by Tukey's multiple comparisons test, AGC: *Ageratum conyzoides* PCOS: Polycystic ovary syndrome.

3.10. Ovarian follicular count

The number of Graafian and corpora lutea follicles decreased significantly in the PCOS relative to the normal control group ($p < 0.05$). There was a significant increase in Graafian and corpora lutea follicles in AGC and PCOS + AGC groups compared to the PCOS group ($p < 0.05$) but the AGC group presented an insignificant higher value of the number of Graafian and corpora lutea follicles than the PCOS + AGC group ($p > 0.05$) [Fig. 6].

The number of cystic and atretic follicles increased significantly in the PCOS group as compared to the normal control group. Post-treatment with AGC reduced the number of cystic and atretic follicles significantly ($p < 0.05$) as compared with the PCOS group. Furthermore, treatment with only AGC exhibited an insignificant reduction in the number of cystic and atretic follicles as compared to the PCOS + AGC group [Fig. 6].

No cystic follicles were identified in the ovaries of normal control animals. However, in the ovaries of animals in the PCOS group, the number of cystic follicles was significantly higher compared to the control ($p < 0.05$). Notably, the number of cystic follicles decreased significantly following post-treatment with AGC, in comparison with the PCOS group. No significant difference was observed in the number of cystic follicles between AGC and PCOS + AGC treatment groups ($p > 0.05$) [Fig. 6].

3.11. Morphometry of antral follicles

When compared to the control group, the PCOS group had a significant increase ($p < 0.05$) in the diameter of antral follicles and the thickness of the theca layer. The thickness of the granulosa layer, on the other hand, decreased significantly ($p < 0.05$). In comparison to the PCOS group, the diameter of the antral follicle and theca layer reduced after treatment with AGC, whereas the diameter of the granulosa increased ($p < 0.05$). There was no significant change in theantral follicle diameter, theca layer, and granulosa diameter between the control, AGC, PCOS + AGC treated groups ($p > 0.05$) [Fig. 7].

3.12. Histomorphology of the ovary

Normal ovarian morphology with mature follicles (tertiary and Graafian follicles) and corpora lutea, which is a sign of ovulation, can be seen in photomicrographs of the ovarian sections of the normal control group [Fig. 8A].

The presence of cystic and atretic follicles dominated the micro-architecture of the ovarian sections of PCOS animals (PCOS group) [Fig. 8B].

Normal ovarian morphology with mature follicles (tertiary and Graafian follicles) and corpora lutea, which is a sign of ovulation, can be seen in photomicrographs of the AGC group's ovarian sections [Fig. 8C].

The ovarian sections of the PCOS + AGC group revealed typical ovarian morphology, including mature follicles, corpora lutea, and a few cystic and atretic follicles [Fig. 8D].

3.13. Histomorphology of the uterus

Photomicrographs of uterine sections from the control group featured normal morphology with a tall cuboidal epithelial outline

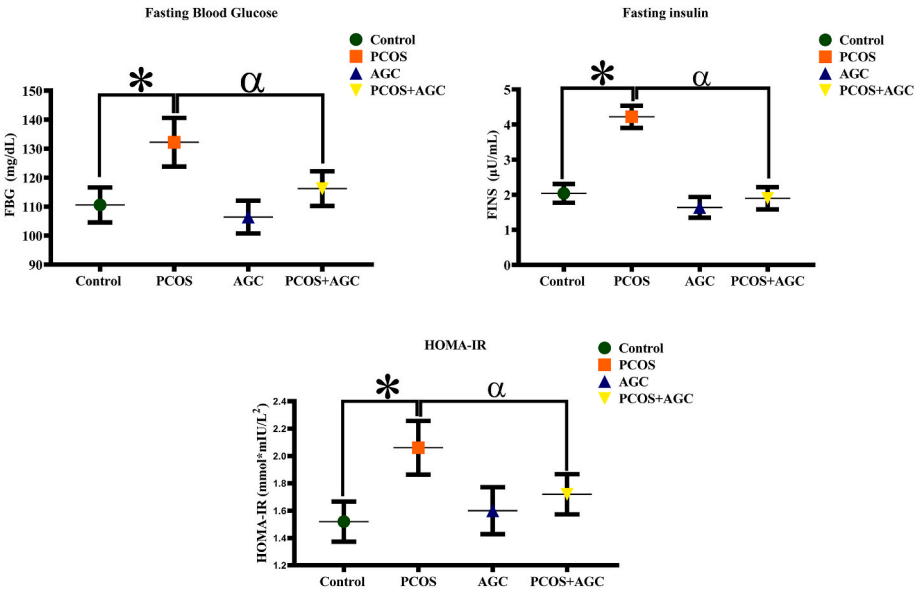

Fig. 4. Effects of *Ageratum conyzoides* extract *on* FBG, FINS, and HOMA-IR in Polycystic ovary syndrome rats. Data presented as mean ± S.E.M, n = 6 in each group, *: represent a significant difference from control, α: represents a significantly different from PCOS at $p < 0.05$, One-Way ANOVA. Follow by Tukey's multiple comparisons test, AGC: *Ageratum conyzoides* PCOS: Polycystic ovary syndrome.

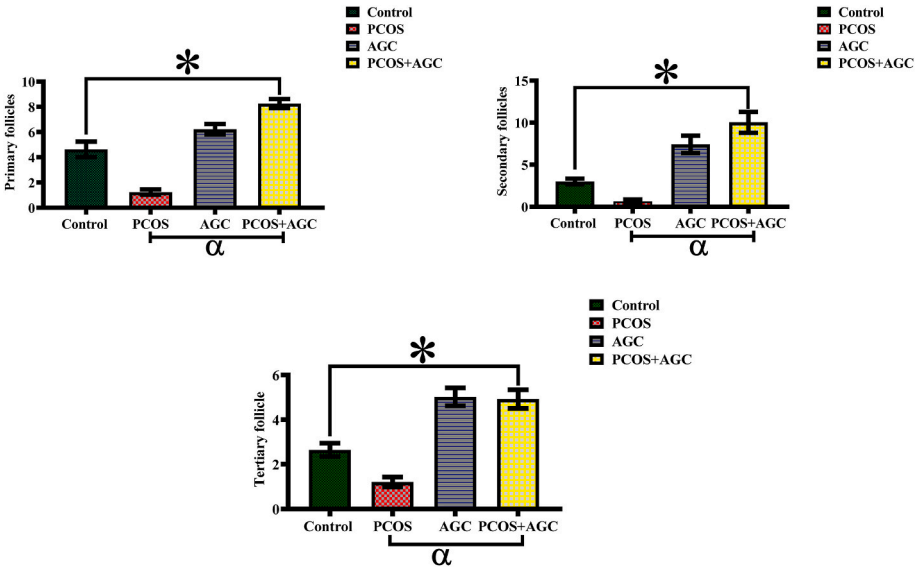

Fig. 5. Effects of *Ageratum conyzoides* extract on the primary, secondary and tertiary follicular count in polycystic ovary syndrome rats. Data presented as mean ± S.E.M, n = 6 in each group, *: represent a significant difference from control, α: represent a significant difference from PCOS at $p < 0.05$, One-Way ANOVA. Follow by Tukey's multiple comparisons test, AGC: *Ageratum conyzoides* PCOS: Polycystic ovary syndrome.

[Fig. 9A].

Photomicrographs of uterus sections from PCOS rats showed degenerated uterine tissue bordered by a poor cuboidal epithelium [Fig. 9B].

Normal morphology with a tall cuboidal epithelial shape may be seen in photomicrographs of uterine sections from the AGC group [Fig. 9C].

Photomicrographs of uterus sections from the PCOS + AGC group indicate changes in uterine epithelial cell shape, with uterine epithelial cells becoming cylindrical and uterine epithelial cells hypertrophy [Fig. 9D].

3.14. Uterine histomorphometric parameters

Morphometric measurements in a section of the uterus of the PCOS rats showed a significant reduction in epithelial height, length of the uterine, endometrium thickness, and numbers of the endometrial gland respectively compared to the control group ($p < 0.05$). However, AGC and PCOS + AGC experimental groups displayed a significant increase ($p < 0.05$) in epithelial height, length of the uterine, endometrium thickness, and numbers of the endometrial gland compared to the PCOS group. The mean value of epithelial height, length of the uterine, endometrium thickness, and numbers of the endometrial gland in AGC and PCOS + AGC treatment groups showed no significant difference ($p > 0.05$) [Fig. 10].

There was observed a significantly higher value in the numbers of

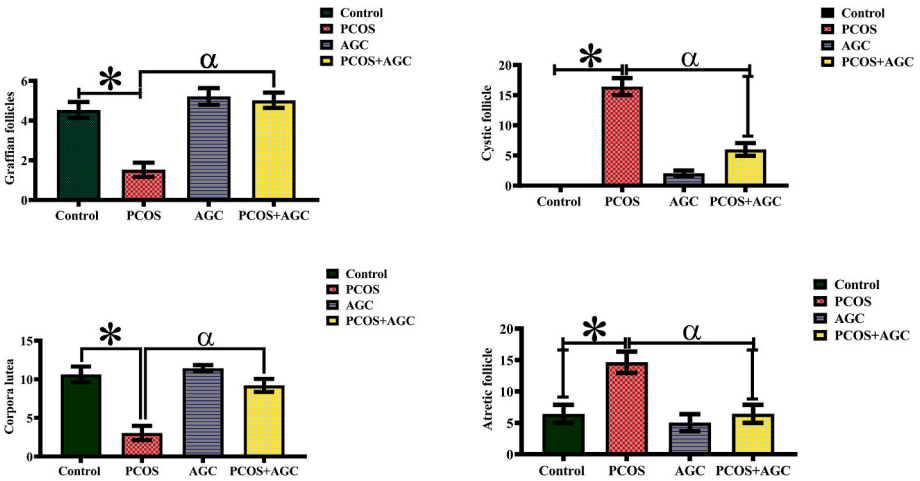

Fig. 6. Effects of *Ageratumconyzoides*extracton ovarian follicle count in polycystic ovary syndrome rats. Data presented as mean ± S.E.M, n = 6 in each group, *: represent a significant difference from control, α: represent a significant difference from PCOS at $p < 0.05$, One-Way ANOVA. Follow by Tukey's multiple comparisons test, AGC: *Ageratum conyzoides* PCOS: Polycystic ovary syndrome.

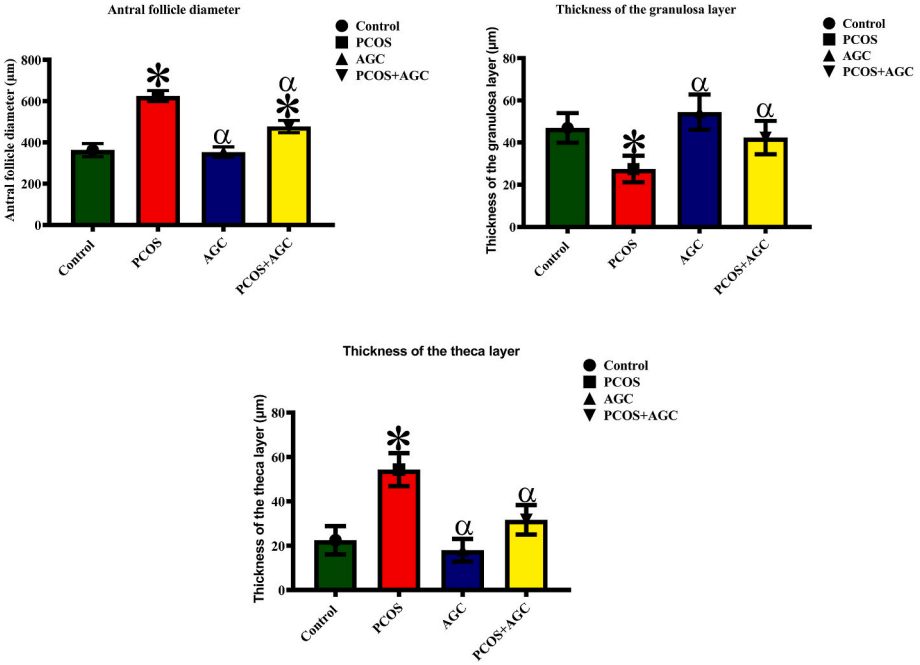

Fig. 7. Effects of *Ageratum conyzoides* extract on morphometry of antral follicles in polycystic ovary syndrome rats. Data presented as mean ± S.E.M, n = 6 in each group, *: represent a significant difference from control, α: represent a significant difference from PCOS at $p < 0.05$, One-Way ANOVA. Follow by Tukey's multiple comparisons test, AGC: *Ageratum conyzoides* PCOS: Polycystic ovary syndrome.

eosinophil cells in the uterine stroma in PCOS rats as compared to the control. But, reduced significantly after treatment with AGC compared to the PCOS group. The group treated with AGC alone also shows a significant reduction in the numbers of eosinophil cells compared to the PCOS group ($p < 0.05$) [Fig. 10].

4. Discussion

In this study, the estrous cycle was disrupted as a result of the EV injection, which increased body weight, BMI, and Lee's index. Throughout the trial period, Lee's index (LI) values for the PCOS group were greater than 310, demonstrating the effectiveness of EV in the induction of PCOS. The significant difference between the initial and final BMI in PCOS rats corroborated the findings of Dadachanji et al. [65], Neubronner et al. [66], and Wang et al. [67].

Ageratum conyzoides intervention reduced the mean BMI and LI, corroborating reports that a little weight loss of about 5% can improve insulin resistance, hormone levels, menstrual cycles, and infertility in women with PCOS [68]. Also, in the AGC and PCOS + AGC therapy groups, there was a decrease in HOMA-IR and an improvement in estrous cyclicity, validating AGC's insulin-sensitizing ability. Marvel et al. [69] and Dou et al. [70] both reported that insulin sensitizers may enhance menstrual cyclicity and ovulation in PCOS patients. Obesity and abdominal obesity aggravate the symptoms of menstruation irregularity and infertility, and are linked to higher levels of androgens and luteinizing hormones in the blood [71]. In both women with PCOS and controls, an increase in body weight is linked to an increase in androgen levels [72]. In the etiology and pathophysiology of PCOS, a complicated connection occurs between obesity, abdominal obesity, insulin resistance, androgen level, and LH level [73]. Elevated body weight and the

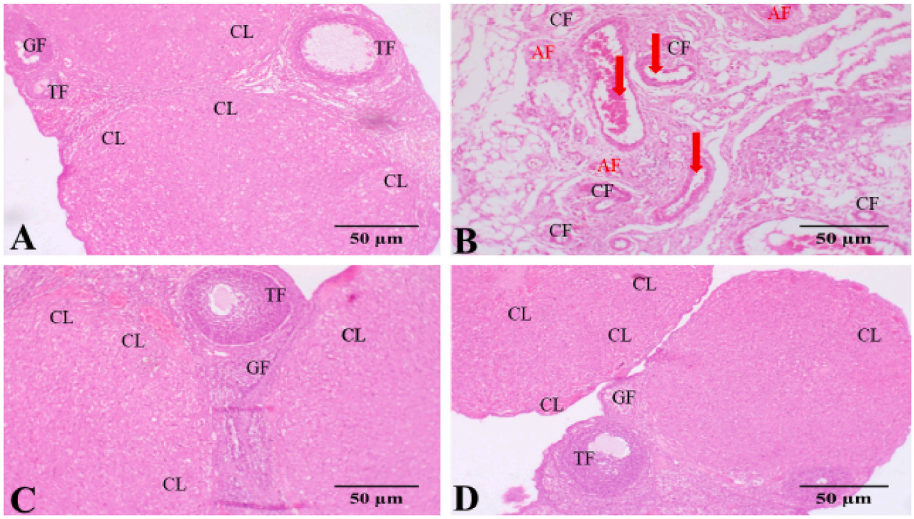

Fig. 8. Photomicrographs of the ovarian cross-section. A: Control group displaying normal histological appearance with corpus luteum (CL) and several healthy follicles. B: Ovarian cross-sections of PCOS group showing many cystic follicles (CF) with lesser CL and healthy follicles. C: Ovarian Section of AGC group showing normal follicles with abundant CL and healthy follicles. D: Section of the PCOS + AGC group revealed improvement in the histological features with the absence of cystic follicles (CF) and the number of luteal bodies and follicles in different stages increased. Stained with [hematoxylin-eosin (H&E) Scale bar-50µm].

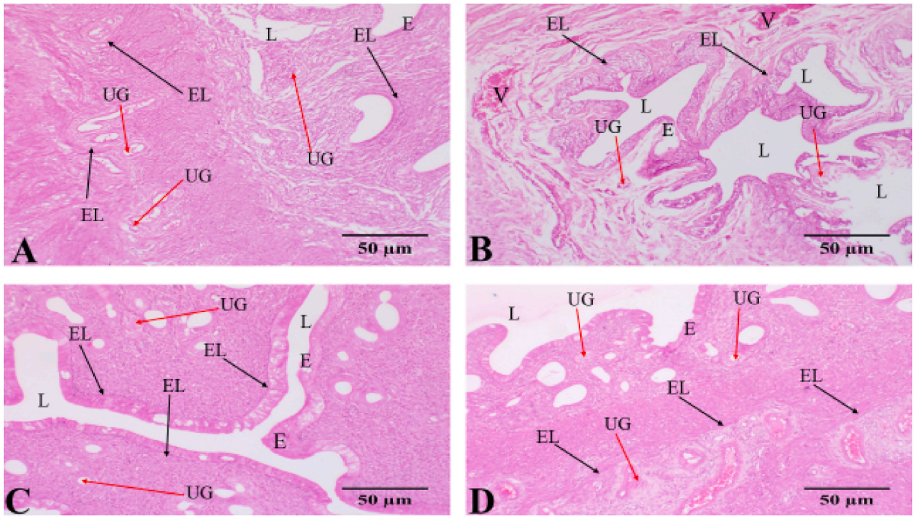

Fig. 9. Photomicrograph of A: control showed normal simple cuboidal epithelial cells lining the uterine gland, and well-pigmented endometrial cells, B: PCOS revealed severe uterine cellular distortion, C: AGC, shows normal histological appearance with normal endometrium lining (EL), and uterine gland (UG) D: PCOS + AGC displaying an improvement in the histological structures with visible endometrium lining (EL), thick uterus and uterine gland almost comparable with the control group. Stained with [Hematoxylin & eosin, Scale bar- 50 µm]. E; Epithelium, L: lumen, UG: uterine glands, EL: Endometrial lining.

presence of estrous cycle anomalies in rats following oral administration of EV injection imply the development of PCOS in rats due to increased androgen and LH hormone levels in our study. When compared to the PCOS group, the AGC and PCOS + AGC therapy groups showed a considerable reduction in body weight. After induction of PCOS, treatment with AGC decreased fat buildup and increased ovarian and uterine weight. Also, AGC caused the estrous cycle to resume after it had been stopped in the diestrus phase following EV injection. This might be connected to lower blood testosterone and LH levels and higher estradiol levels, which would benefit ovarian follicular growth and maturation, follicle atresia reduction, and corpora lutea formation and maintenance. We may assume that the bioactive component of AGC has overcome the inhibitory effect of EV, resulting in lower levels of testosterone and LH and higher levels of progesterone and estradiol. The progesterone and estradiol would have accelerated the proliferation of uterine epithelial cells. This uterotrophic effect is known to be mediated by estrogen receptor alpha [74]. Furthermore, because AGC reduced circulating free androgen, the improvement in ovarian dynamic indicated that AGC reduced androgen stimulation of insulin release by pancreatic cells. Hyperinsulinemia caused by hyperandrogenism has been linked to early granulosa cell maturation and luteinization, follicular growth arrest, anovulation, and cyst development [75]. Low levels of high-density lipoprotein cholesterol (HDL-C), high levels of triglycerides, total cholesterol, and low-density lipoprotein cholesterol (LDL-C) are all common symptoms of the polycystic ovarian syndrome [76].

Although extensive series of data shows that the mean circulating lipid levels in women with PCOS are within acceptable limits, up to 70% of individuals have at least one aberrant lipid level [77].

In our study, the levels of glucose, cholesterol, and triglyceride levels in PCOS rats were all considerably higher. However, after treatment with AGC, the levels of glucose, cholesterol, and triglycerides all decreased dramatically. In PCOS rats, there was a considerable rise in LDL-C and VLDL-C. However, in the PCOS group, HDL-C levels are considerably lower than in the control group. The activation of the hormone-sensitive lipase in PCOS rats was mostly due to an increase in the release of fatty acids from peripheral tissue to the blood vessels, which might be attributable to an increase in the release of fatty acids from peripheral tissue to the blood vessels. As a result, treatment with AGC following PCOS induction raises HDL-C while lowering VLDL-C and HDL-C. The considerable fall in glucose levels following AGC administration might be due in part to the bioactive components of AGC promoting glucose entrance into cells, hence reducing glucose release into the bloodstream. Finally, it appears that AGC extracts affect the metabolic complication of PCOS (dyslipidemia). Carani et al. [78] and Orostica et al. [79] reported that inflammation is activated and increased in different endometrial cells and the serum of PCOS patients,

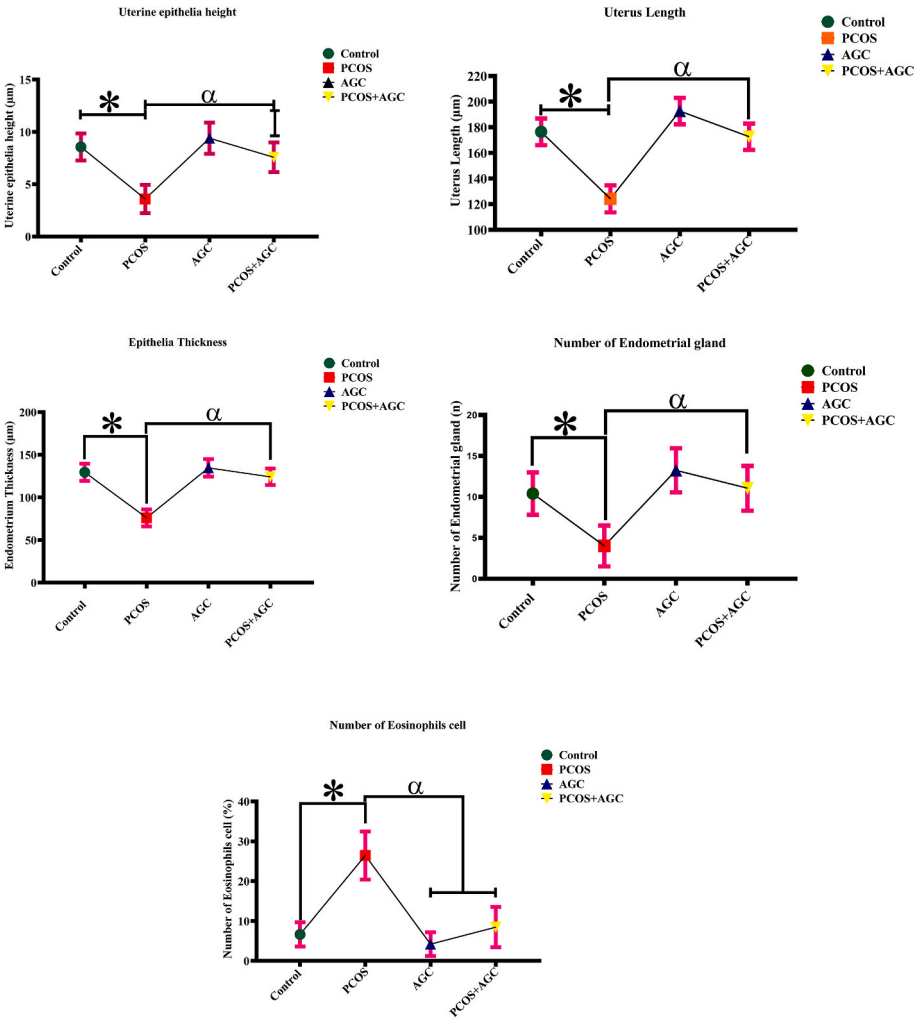

Fig. 10. Effects of *Ageratum conyzoides* extract on uterine morphometry parameters in polycystic ovary syndrome rats. Data presented as mean ± S.E.M, n = 6 in each group, *: represent a significant difference from control, α: represents a significantly different from PCOS at $p < 0.05$, One-Way ANOVA. Follow by Tukey's multiple comparisons test, AGC: *Ageratum conyzoides* PCOS: Polycystic ovary syndrome.

and the current study shows that the expression of an array of inflammation-related markers is dramatically altered in the PCOS-like rat uterus. TNF and IL-6 levels in the uterus are enhanced in PCOS-like mice, indicating that TNF and IL-6 have an inflammatory role in endometrial function in PCOS patients [80]. Low-grade inflammation has been linked to PCOS [81], which supports the current findings, which reveal that serum IL-6, IL-18, TNF-, and CRP levels are considerably higher in PCOS rats. The anti-inflammatory activity of AGC, which improved the low-grade inflammation state and downregulated pro-inflammatory cytokine production (TNF-α, IL-18, and IL-6) in this study, might explain why AGC intervention dramatically reduced the levels of inflammation components in PCOS rats. The imbalance between oxidants and antioxidants, as well as the increased creation of reactive oxygen species (ROS), is referred to as oxidative stress [82,83]. In PCOS, the production of reactive oxygen species (ROS) by mononuclear cells (MNCs) in response to hyperglycemia increased, regardless of weight [84]. In PCOS, oxidative indicators in the bloodstream are much higher, and oxidative stress plays a key role in PCOS pathogenesis [85].

In this study, ovarian SOD, CAT, and total peroxidase concentrations were much lower in PCOS rats, whereas ovarian MDA was significantly greater in PCOS rats, which was consistent with earlier research on PCOS patients [86,87]. In this paradigm, oxidative stress was verified in PCOS rats. In comparison to control rats, post-treatment with AGC dramatically increased ovarian SOD, CAT, and total peroxidase and decreased ovarian MDA. This might be related to AGC's antioxidant ability, which mops up free radicals and reduces ROS. As a result, we may conclude that AGC is efficient in reducing oxidative stress and improving the antioxidant system in the PCOS rat model.

Endometrial deficiencies may be the cause of implantation failure in PCOS patients, as evidenced by dysregulation of the expression of proteins necessary for implantation in the human endometrium [88]. AGC therapy restores endocrine (hyperandrogenism), metabolic (insulin resistance), and reproductive (lack of estrous cycle) problems, as well as partially reverses implantation failure in most PCOS-like rats, according to our findings. It has been discovered that several chemicals in the uterus are essential for implantation and that mutations in these molecules result in infertility [89]. In addition, investigations have shown that in PCOS individuals, endometrial decidualization is hindered [90].

In this study, histological studies of uterine tissue sections of PCOS rats revealed a considerable increase in uterine wall thickness and epithelial height as compared to the control group. It has been demonstrated that estrogen-mediated uterine stimulation causes morphogenetic changes, such as changes in the kind and shape of luminal and glandular epithelia [91]. *In vitro*studies of radiothymidine uptake by endometrium suggest that high levels of estradiol are primarily associated with maximal proliferation in uterine glands and stroma [92], and that ovarian steroids are among the most important factors that affect

uterine morphology and motility [93,94].

The findings of this study also backed up the theory that an aberration in ovarian steroids causes obvious alterations in the epithelial surface, gland accumulation, and overall thickness of the uterine wall. In addition, an increase in eosinophil quality in the endometrial stroma in PCOS rats was detected in the current study, confirming a valuable report that PCOS increases eosinophil quality in the uterine stroma [95]. The influence of hormonal changes on reproductive tissues revealed that leukocyte entry into uterine tissues is mostly controlled by hormones [96]. PCOS has been shown to cause histo-architectural abnormalities in the ovary [97] and uterine of rats [98].This study found that PCOS rats have the leastcorpus luteum and numerous follicular ovarian cysts, which is consistent with animal models of PCOS [99,100]. Reduced levels of testosterone, FSH, LH, and antioxidant activity might be linked to decreased ovarian weight, uterine length and weight, endometrium thickness, and endometrial gland numbers. In the AGC and PCOS + AGC therapy groups, there wereincrease in corpora lutea numbers, ovarian and uterine weight, endometrium thickness, and endometrial gland numbers, as well as a decrease in cystic follicle counts. The presence of corpora lutea indicates that the animals have ovulated [101].

Higher levels of progesterone in AGC post-treated rats and rats treated with AGC alone indicated the occurrence of ovulation, indicating that AGC had restored ovulation in the PCOS rats. This is significant because the primary goal of PCOS care is to restore ovulation. The favorable effect of AGC on the histomorphology and histomorphometry of the uterus and ovaries might be due to the high antioxidant, anti-inflammatory, and pro-fertility effects of the bioactive component of AGC. Treatment with AGC resulted in substantial improvements in testosterone, estrogen, LH levels, and ovarian and uterine tissue. The histological findings in the AGC-treated group revealed a significant recovery of ovarian tissue, with the existence of several follicles in various stages of development, indicating normal oogenesis. The granulosa layer was normal, with distinct thecal layers in the follicles. The existence of corpora lutea following AGC therapy demonstrated that AGC treatment restored the normal estrous cycle. *AGC* had an anti-androgenic effect, lowering androgen levels and preventing ovarian cell malfunction in PCOS patients, resulting in improved fertility [102]. AGC's success in the treatment of PCOS may be due to the observed healing of ovarian tissue as well as its antiandrogen capability. This study has several limitations. First, the levels of TNF-α, IL-6 and IL-18 expression were not identified. Second, ovarian cell count and uterine histomorphometric took several weeks to establish and were very time-consuming. Third, leptin and Anti-Müllerian hormone were not verified in this study. In the next step, metformin or other insulin sensitizers and combination of metformin and*Ageratum conyzoides* will be used to treat PCOS rats to verify the changes of the insulin signaling pathway or to assess new therapeutic methods in this model.

5. Conclusion

Infertility is a serious worry for PCOS patients, and follicular atresia, anovulation, and subsequent hyperandrogenemia are common causes of infertility. Phytotherapy is gaining popularity due to perceived low cost, availability, efficacy and few side effects. This is more prominent in low-income countries of the world. *Ageratum conyzoides* can be utilized to treat infertile individuals whose infertility is caused by low oocyte quality and anovulation. We find that *Ageratum conyzoides* can improve insulin sensitivity, lipid profile, antioxidant activity, hormonal balance, and anti-inflammatory activity in female rats, thus reversing the symptoms of PCOS. These findings add to our existing knowledge of the possible use of *Ageratum conyzoides* as an antioxidant for the treatment of PCOS and as an alternative therapy for the treatment of PCOS.

Funding

This study got no particular support from the government, commercial, or non-profit funding entities. It was carried out as part of the authors' obligation and condition of services at the Animal Facility of the School of Basic Medical Science, Federal University of Technology, Akure, Nigeria.

Availability of data and materials

All data generated or analyzed during this study are included in this manuscript.

CRediT authorship contribution statement

Sunday Aderemi Adelakun: Conceptualization, Methodology, Validation, Writing – review & editing, Investigation, Writing – original draft. **Victor Okoliko Ukwenya:** Formal analysis, Investigation, Writing – original draft. **Akwu Bala Peter:** Methodology, Project administration, Supervision, Investigation. **Adewale Jacob Siyanbade:** Writing – original draft, Investigation. **Comfort Oluwakorede Akinwumiju:** Writing – original draft, Investigation.

Declaration of competing interest

The authors declare that they have no competing interests.

Acknowledgments

Material support was provided by the Department of Human Anatomy at the Federal University of Technology, Akure, Nigeria. Mr. Ige of the Histology Laboratory, Department of Anatomy and Cell Biology, Obafemi Awolowo University, Ife, Nigeria, who performed the histological procedure, Mr. Adewole, who determined hormones in serum samples, Dr. Tosan, who determined oxidative stress-related parameters in ovary homogenates, and Mr. Omomoh Bernard, who identified the plant material, deserve special thanks. Adebayo T. Adedolapo, Afolabi Maryam, and Adisa DamilolaObanijesu are among the many undergraduate members of our laboratory who have dedicated themselves to animal care and husbandry.

References

[1] Bannigida DM, Nayak BS, Vijayaraghavan R. Insulin resistance and oxidative marker in women with PCOS. Arch Physiol Biochem 2020;126(2):183–6.
[2] MdMoin AS, Sathyapalan T, Atkin SL, Butler AE. Renin-Angiotensin System over activation in polycystic ovary syndrome, a risk for SARS-CoV-2 infection? Metab. Open 2020;7:100052.
[3] MdMoinAS, Sathyapalan T, Butler AE. The relationship of soluble neuropilin-1 to severe COVID-19 risk factors in polycystic ovary syndrome. Metab. Open 2021;9:100079.
[4] Haqshah MZ, Shrivastava VK. Turmeric extract alleviates endocrine-metabolic disturbances in letrozole-induced PCOS by increasing adiponectin circulation: a comparison with Metformin. Metab. Open 2022;13:100160.
[5] Sui L, Yan K, Zhang H, Nie J, Yang X, XuC L, et al. Mogroside V alleviates oocyte meiotic defects and quality deterioration in benzo(a)pyrene-exposed mice. Front Pharmacol 2021;12:722779.
[6] Cabus U, Kabukcu C, Fenkci S, Caner V, Oztekin O, Fenkci V, Enli Y. Serum caspase-1 levels in women with polycystic ovary syndrome. Taiwan J Obstet Gynecol 2020;59(2):207–10.
[7] Saei G, Naz M, Ramezani TF, Behroozi-Lak T, Mohammadzadeh F, Kholosi BF, et al. Polycystic ovary syndrome and pelvic floor dysfunction: a narrative review. Res Rep Urol 2020;12:179–85.
[8] Liang A, Huang L, Liu H, He W, Lei X, Li M, et al. Resveratrol improves follicular development of PCOS rats by regulating the glycolytic pathway. MolNutr Food Res 2021;65(24):e2100457.
[9] Barrea L, Frias-Toral E, Verde L, Cucalón G, Ceriani F, Garcia-Velasquez E, et al. PCOS and nutritional approaches: differences between lean and obese phenotype. Metab. Open 2021;(12):100123. 2021.
[10] Huang L, Liang A, Li T, Lei X, Chen X, Liao B, et al. Mogroside V improves follicular development and ovulation in young-adult PCOS rats induced by letrozole and high-fat diet through promoting glycolysis. Front Endocrinol 2022;13:838204.
[11] Wang D, Weng Y, Zhang Y, Wang R, Wang T, Zhou J, et al. Exposure to hyperandrogen drives ovarian dysfunction and fibrosis by activating the NLRP3 inflammasome in mice. Sci Total Environ 2020;745:141049.

[12] Nie J, Yan K, Sui L, Zhang H, Zhang H, Yang X, et al. Mogroside V improves porcine oocyte *in vitro* maturation and subsequent embryonic development. Theriogenology 2020;141:35–40.
[13] Zhang HL, Yi M, Li D, Li R, Zhao Y, Qiao J. Tran generational inheritance of reproductive and metabolic phenotypes in PCOS rats. Front Endocrinol 2020;11:144.
[14] Nejabati HR, Samadi N, Shahnazi V, Mihanfar A, Fattahi A, Latifi Z, et al. Nicotinamide and its metabolite N1-methylnicotinamide alleviate endocrine and metabolic abnormalities in adipose and ovarian tissues in rat model of polycystic ovary syndrome. Chem Biol Interact 2020;324:109093.
[15] Dumesic DA, Padmanabhan V, Chazenbalk GD, Abbott DH. Polycystic ovary syndrome as a plausible evolutionary outcome of metabolic adaptation. Reprod Biol Endocrinol RB&E 2022;20(1):12.
[16] Kotta JC, Lestari ABS, Candrasari DS, Hariono M. Medicinal effect, in silico bioactivity prediction, and pharmaceutical formulation of *Ageratum conyzoides* L.: a review. Sci Tech Rep 2020;6420909:1–12.
[17] Ukwenya VO, Adelakun SA, Elekofehinti OO. Exploring the antidiabetic potential of compounds isolated from Anacardiumoccidentale using computational aproach: ligand-based virtual screening. Silico Pharmacol 2021;9(1):1–16.
[18] Omotoso OD, Adelakun SA, Amedu NO, Idoko UP, Oji IS, Akpan HB. PAS exfoliation in watermelon and aloe vera recuperate glycogen in heart tissue damaged by cadmium in adult wistar rats (*rattusnovergicus*). Cardiology and angiology. Int J 2016;5(3):1–8.
[19] Olawuyi TS, Akinola BK, Adelakun SA, Ogunlade BS, Akingbade GT. Effects of aqueous leaf extract of *lawsoniainermis* on aluminuminduced oxidative stress and adult wistar rat pituitary GlandHistology. JBRA Assist Reprod 2019;23(2):117–22.
[20] Gangsheng W. Traditional Chinese medicine composition for preparing Candida resisting medicines. China patent application No. 104083361A, 2 march 2016. Available online: https://patents.google.com/patent/CN104083361A/en. [Accessed 10 April 2022].
[21] Adelakun SA, Akingbade GT, Aniah JA, Modupeoluwa OO. Histomorphological and biochemical assessment of testicular parameters following oral administration of cadmium nitrate to adult male wistar rats. Eur J Biomed Pharmaceut Sci 2017;4(6):36–43.
[22] Akang EN, OremusuAA, Osinubi AA, Dosumu OO, Kusemiju TO, Adelakun SA, et al. Histomorphometric studies of the Impact of *Telfaira occidentalis* on Alcohol-induced Gonado- toxicity in male rats. Toxicol Rep 2015;2:968–75.
[23] Falade MJ, Borisade OA, Aluko M. Evaluation of antifungal activities of five plant extracts against *pseudoperenosporacubensis* (downy mildew) in muskmelon (*cucumismelo* L.). Annu Res Rev Biol 2019;31:1–6.
[24] Budiman A, Aulifa DL. A study comparing antibacterial activity of *Ageratum conyzoides* L. Extract and *Piper betle* L. Extract in gel dosage forms against *Staphylococcus aureus*. Phcog J 2020;12:473–7.
[25] Permawati M, Anwar E, Arsianti A, Bahtiar A. Anti-inflammatory activity of nanoemulgel formulated from *Ageratum conyzoides* (L.) l. And *Oldenlandiacorymbosa* l. Extracts in rats. J Nat Remedies 2019;19:124–34.
[26] Adesanwo JK, Egbomeade CO, Moronkola DO, Akinpelu DA. Chemical, toxicity and antibacterial studies on methanol extracts of *melantherascandens, Ageratum conyzoides, aspiliaafricana*, and *synedrellanodiflora*. J Explor Res Pharmacol 2019;4:1–7.
[27] Luo Z, Chen X, Xia G, Chen X. Extrinsic environmental factors, not resident diversity itself, lead to the invasion of *Ageratum conyzoides* L. in diverse communities. Ecol Res 2018;33(6):1245–53.
[28] Paul S, Datta BK, Ratnaparkhe MB, Dholakia BB. Turning waste into beneficial resource: implication of *Ageratum conyzoides* L. In sustainable agriculture, environment and biopharma sectors. Mol Biotechnol 2022;64:221–44.
[29] Negi B, Bargali SS, Bargali K, Khatri K. Allelopathic interference of *Ageratum conyzoides* L. against rice varieties. Curr Agri Res 2020;8(2):69–76.
[30] Chahal R, Nanda A, Akkol EK, Sobarzo-Sánchez E, Arya A, Kaushik D, et al. Ageratum conyzoides L. And its secondary metabolites in the management of different fungal pathogens. Molecules 2021;26:2933.
[31] Qiao Z, Chen Z, Wang Q. The complete chloroplast genome of Ageratum conyzoides (Asteraceae). Mitochondrial DNA Part B 2019;4(2):3342–3.
[32] Patil A, Kishore K, Arya M, Shivani. Phytochemical screening of *Ageratum conyzoides* and its antimicrobial activity against staphylococcus aureus and Escherichia coli. Int J Res Anal Rev 2019;6(2):312–20.
[33] Ojewale AO, Akpan HB, Faduyile FA, Shallie PD, Akande AA, Adefule AK. Hepatoprotective activities of ethanolic roots extract of *Ageratum conyzoides* on alloxan-induced hepatic damage in diabetic wistar rats. J Morphol Sci 2019;36(1):39–45.
[34] Akpan HB, Omotoso OD, Ogbonna E, Negedu MN, Adelakun SA, Oladipupo FE, et al. Histo-morphological effects of *Carica papaya* on cadmium induced prefrontal-cortex damage in adult wistar rats. Eur J Med Plants 2018;23(3):1–10.
[35] Adelakun SA, Ukwenya VO, Akingbade GT, Omotoso OD, Aniah JA. Interventions of aqueous extract of *Solanum melongena* fruits (garden eggs) on mercury chloride-induced testicular toxicity in adult male Wistar rats. Biomed J 2020;43(2):174–82.
[36] Soni A, Sosa. Phytochemical analysis and free radical scavenging potential of herbal and medicinal plant extracts. J Pharmacogn Phytochem 2013;2:22–9.
[37] Grindberg T, Williams K. Vitamin C quantification using reversed-phase ion pairing HPLC. Concordia Coll J Anal Chem 2010;1:19–23.
[38] Akubugwo IE, Obasi NA, Chinyere GC, Ugbogu AE. Mineral and phytochemical contents in leaves of Amaranthushybridus L. and Solanum nigrum L. were subjected to different processing methods. Afr J Biochem Res 2008;2:40–4.
[39] National Research Council. Guide for the care and the use of laboratory animals, 20. Bethesda: National Institute of Health; 1985. 85–23.
[40] Adelakun S, Omotoso O, Aniah J, Oyewo O. Seneciobiafrae defeated tetracycline-induced testicular toxicity in adult male Sprague Dawley rats. JBRA Assist Reprod 2018;22(4):314–22.
[41] Kulkarni SK. Hand book of experimental pharmacology. 1999. New Delhi, India.
[42] Wu C, Lin F, Qiu S, Jiang Z. The characterization of obese polycystic ovary syndrome rat model suitable for exercise intervention. PLoS One 2014;9(6):e99155.
[43] Mamikutty N, Thent ZC, Sapri SR, Sahruddin NN, Mohd YMR, Haji SF. The establishment of metabolic syndrome model by induction of fructose drinking water in male Wistar rats. BioMed Res Int 2014;263897:1–8.
[44] Adelakun SA, Ogunlade B, Fidelis OP, Omotoso OD. Protective effect of nutritional supplementation of zinc-sulfate against cisplatin-induced spermatogonial and testicular dysfunctions in adult male Sprague- Dawley rats. Endocr metab Sci 2021;5:100116.
[45] Arika WM, Kibiti CM, Njagi JM, Ngugi MP. Modulation of cognition: the role of gnidiaglauca on spatial learning and memory retention in high fat diet-induced obese rats. Neural Plast 2019;2867058:1–16.
[46] Nurdiana S, Goh YM, Hafandi A, Dom SM, NurSyimal'ain A, Noor Syafnaz NM, et al. Improvement of spatial learning and memory, cortical gyrification patterns and brain oxidative stress markers in diabetic rats treated with Ficusdeltoidea leaf extract and vitexin. J Tradit Complement Med 2017;8(1). 190–02.
[47] Shen HR, Xu X, Li XL. Berberine exerts a protective effect on rats with polycystic ovary syndrome by inhibiting the inflammatory response and cell apoptosis. Reprod Biol Endocrinol 2021;19:3.
[48] Adelakun SA, Ogunlade B, Fidelis OP, Adedotun OA. *Cyprus esculentus* suppresses hepato-renal oxidative stress, inflammation, and caspase-3 activation following chronic exposure to sodium fluoride. Phytomedicine 2022;2:100163.
[49] Adelakun SA, Ogunlade B. Responses to the bioactive component of crassocephalumcrepidioides on histomorphology, spermatogenesis and steroidogenesis in streptozotocin-induced diabetic male rats. J Reprod Endocrinol. Infert. 2018;3(1):6.
[50] Adelakun SA, Akintunde OW, Jeje SO, Alao OA. Ameliorating and protective potential of 1-isothiocyanato-4-methyl sulfonyl butane on cisplatin-induced oligozoospermia and testicular dysfunction via redox-inflammatory. Phytomedicine 2022:100268.
[51] Friedewald WT, Lewis RT, Fredrickson DS. Estimation of the concentration of Low-Density Lipoprotein cholesterol in plasma without use of the preparative ultracentrifuge. Clin Chem 1972;18. 499–02.
[52] Wilbur K, Bernhein F, Shapiro O. Determination of lipid peroxidation. Arch Biochem Biophys 1949;24:3959–64.
[53] Adelakun SA, Ukwenya VO, Ogunlade BS, Aniah JA, Ibiayo AG. Nitrite-induced testicular toxicity in rats: therapeutic potential of walnut oil. JBRA Assist Reprod 2019;23(1):15–23.
[54] Asada K, Takahashi M, Nagate M. Assay and inhibitors of spinach superoxide dismutase. Agric Chem 1974;38:471–3.
[55] Sinha KA. Colorimetric assay of catalase. Anal Biochem 1972;47:389–94.
[56] Habbu P, Shastry R, Mahadevan K, Hanumanthachar J, Das S. Hepatoprotective and antioxidant effects of argyreiaspeciosa in rats. Afr J Tradit, Complementary Altern Med 2008;5(2):158–64.
[57] Omotoso OD, Adelakun SA, Akwu BP, Ogbonna E, Idomeh IJ. Histochemical assessment of Moringa–oleifera oil and walnut oil on cadmium induced lateral geniculate body damage in developing male Wistar rats (Rattusnovergiccus). Anatomy J Africa 2019;8(2). 1593-05.
[58] Servais S. Altérationmitochondriale et stress oxydantpulmonaireenréponse à l 'ozone :effet de l 'âge et d 'unesuplémentationen oméga-3, 1. Lyon: Thèse de doctorat de l 'université Claude Bernard; 2004. p. 17–40.
[59] Adelakun SA, Ogunlade B, Iteire KA, Adedotun OA. Ameliorating potential and fertility-enhancing activities of nutritional dietary supplementation of D-Ribose –l-Cysteine in cisplatin induced oligoasthenoteratozoospermia and seminiferous epithelium degeneration in adult male Sprague-Dawley rats. Metab open 2021;12:100128.
[60] Oyeniran DA, Ojewale AO, Jewo PI, Ashamu EA, Adeniyi OO, et al. Infertility: a product of smoke emanating from Transfluthrin-coated insecticide paper (TCIP). Toxicol Res Appl 2021;5:1–7.
[61] Akingbade G, Ijomone O, Adelakun S, Enaibe B. Histological and biochemical alterations in the superior colliculus and lateral geniculate nucleus of juvenile rats following prenatal exposure to marijuana smoke. Basic Clin Neurosci 2021;12(6):745–58.
[62] Ogunlade B, Adelakun SA, Ukwenya VO, Elemoso TT. Potentiating response of D-Ribose-L-Cysteine on Sodium arsenate-induced hormonal imbalance, spermatogenesis impairments and histomorphometric alterations in adult male Wistar rat. JBRA Assist Reprod 2021;25(3):358–67.
[63] Ukwenya VO, Olawuyi TS, Adelakun SA, Ogunsola OI, Ukwenya M. D-ribose-L-cysteine improves hormonal imbalance, spermatogenic dysregulation, and redox status in streptozotocin-diabetic rats. Comp Clin Pathol 2020;29(6):1–11.
[64] Adelakun SA, Akintunde OW, Akingbade GT, Adedotun OA. Bioactive component of aqueous extract of Solanum melongena ameliorate estradiol valerate induced ovarian-pituitary dysfunctions in female Sprague–Dawley rats: histomorphological and biochemical evidence. Phytomedice plus 2022;2:100175.
[65] Dadachanji R, Patil A, Joshi B, Mukherjee S. Elucidating the impact of obesity on hormonal and metabolic perturbations in polycystic ovary syndrome phenotypes in Indian women. PLoS One 2021;16(2):e0246862.
[66] Neubronner SA, Indran IR, Chan YH, Thu AWP, Eu-Leong Yong E. Effect of body mass index (BMI) on phenotypic features of polycystic ovary syndrome (PCOS) in

Singapore women: a prospective cross-sectional study. BMC Wom Health 2021; 21:135.
[67] Wang M, Yin Q, Xu X. A rat model of polycystic ovary syndrome with insulin resistance induced by letrozole combined with high fat diet. Med Sci Monit 2020; 26:e922136-1–922136-10.
[68] Ding H, Zhang J, Zhang F, Zhang S, Chen X, Liang W, et al. Resistance to the insulin and elevated level of androgen: a major cause of polycystic ovary syndrome. Front Endocrinol 2021;12:741764.
[69] Merviel P, James P, Bouée S, Le Guillou M, Rince C, Nachtergaele C, et al. Impact of Myo-inositol treatment in women with polycystic ovary syndrome in assisted reproductive technologies. Reprod Health 2021;18:13.
[70] Dou L, Zheng Y, Li L, Gui X, Chen Y, Yu M, et al. The effect of cinnamon on polycystic ovary syndrome in a mouse model. Reprod Biol Endocrinol 2018;16: 99.
[71] Salehi R, Mazier HL, Nivet AL, Reunov AA, Lima P, Wang Q, et al. Ovarian mitochondrial dynamics and cell fate regulation in an androgen-induced rat model of the polycystic ovarian syndrome. Sci Rep 2020;10:1021.
[72] Shahrokhi SA, Naeini AA. The association between dietary antioxidants, oxidative stress markers, abdominal obesity, and poly-cystic ovary syndrome: a case-control study. J ObstetGynaecol 2020;40(1):77–82.
[73] Sherafatmanesh S, Ekramzadeh M, Tanideh N, Golmakani MT, Koohpeyma F. The effects of thylakoid-rich spinach extract and aqueous extract of caraway (*Carumcarvi L.*) in letrozole-induced polycystic ovarian syndrome rats. BMC Complement Med Ther 2020;20:249.
[74] Ndeingang EC, Defo DPB, Watcho P, Kamanyi A. *Phyllanthusmuellerianus* (Euphorbiaceae) restores ovarian functions in letrozole-induced polycystic ovarian syndrome in rats. Evid Based Complement Alternat Med 2019:2965821.
[75] Kim CH, Chon SJ, Lee SH. Effects of lifestyle modification in polycystic ovary syndrome compared to metformin only or metformin addition: a systematic review and meta-analysis. Sci Rep 2020;10:7802.
[76] Kakadia N, Patel P, Deshpande S, Shah G. Effect of Vitexnegundo L. seeds in letrozole induced polycystic ovarian syndrome. J Tradit Complement Med 2019; 9:336–45.
[77] Liu XY, Yang YJ, Tang CL, Wang K, Chen JJ, Teng XM, et al. Elevation of antimüllerian hormone in women with polycystic ovary syndrome undergoing assisted reproduction: effect of insulin. Fertil Steril 2019;111(1):157–67.
[78] Carani A, Dipti N. Sitagliptin recuperates oxidative stress and inflammatory cytokine expression in ovary of PCOS rats. J Drug Deliv Ther 2019;9(4):244–51.
[79] Orostica L, Astorga I, Plaza-Parrochia F, Vera C, Garcia V, Carvajal R, et al. Proinflammatory environment and role of TNF-alpha in the endometrial function of obese women having polycystic ovarian syndrome. Int J Obes 2016;40: 1715–22.
[80] Piltonen TT. Polycystic ovary syndrome: endometrial markers. Best Pract Res Clin Obstet Gynaecol 2016;37:66–79.
[81] Mohammadi S, Karimzadeh BL, Hojati V, Ghorbani AG, Nabiuni M. Anti-inflammatory effects of curcumin on insulin resistance index, levels of interleukin-6, C-reactive protein, and liver Histology in polycystic ovary syndrome-induced rats. Cell J 2017;19(3):425–33.
[82] Ogunlade B, Akunna GG, Fatoba OO, Ayeni OJ, Adegoke AA, Adelakun SA. Aqeous extract of *VernoniaAmygdalina* protects against alcohol induced hepatotoxicity in wistar rats. World J Young Res (WJYR) 2012;2(5):70–7.
[83] Ogunlade B, Adelakun SA, Iteire K. Sulforaphane response on aluminum-induced oxidative stress, alterations in spermcharacterization and testicular histomorphometry in Wistar rats. Int J Reprod BioMed 2020;18:611–24.
[84] Makanjuola VO, Omotoso OD, Fadairo OB, Dare BJ, Oluwayinka P, Adelakun SA. The effect of parkia leaf extract on cadmium-induced cerebral leison in wistar rats. Br J Med Med Res 2016;12(4):1–7.
[85] Mvondo MA, Mzemdem TFI, Awounfack CF, Njamen D. The leaf aqueous extract of *Myrianthusarboreus P. Beauv*. (Cecropiaceae) improved letrozole-induced polycystic ovarian syndrome associated conditions and infertility in female Wistar rats. BMC Complement Med Ther 2020;20:275.
[86] Bandariyan E, Mogheiseh A, Ahmadi A. The effect of lutein and *Urticadioica* extract on *in vitro* production of embryo and oxidative status in polycystic ovary syndrome in a model of mice. BMC Complement Med Ther 2021;21:55.
[87] Haslan MA, Samsulrizal N, Hashim N, Mohamad, Zin NSN, Shirazi FH, Goh YM. Ficusdeltoidea ameliorates biochemical, hormonal, and histomorphometric changes in letrozole-induced polycystic ovarian syndrome rats. BMC Compleme Med Therap 2021;21:291.
[88] George AF, Jang KS, Nyegaard M, Neidleman J, Spitzer TL, Xie G, et al. Seminal plasma promotes decidualization of endometrial stromal fibroblasts in vitro from women with and without inflammatory disorders in a manner dependent on interleukin-11 signaling. Hum Reprod 2020;35:617–40.
[89] Ochoa-Bernal MA, Fazleabas AT. Physiologic events of embryo implantation and decidualization in human and non-human primates. Int J Mol Sci 2020;21(6): 1973.
[90] Eisman LE, Pisarska MD, Wertheimer S, Chan JL, Akopians AL, Surrey MW, et al. Clinical utility of the endometrial receptivity analysis in women with prior failed transfers. J Assist Reprod Genet 2021;38:645–50.
[91] Mirabolghasemi G, Kamyab Z. Changes of the uterine tissue in rats with polycystic ovary syndrome induced by estradiol valerate. Int J Fertil 2017;11(1). 47–5.
[92] Xu J, Dun J, Yang J, Zhang J, Lin Q, Huang M, et al. Letrozole rat model mimics human polycystic ovarian syndrome and changes in insulin signal pathways. Med Sci Monit 2020;26:e923073-1–923073-13.
[93] Rajan RK, Balaji B. Soy isoflavones exert beneficial effects on the letrozole-induced rat polycystic ovary syndrome (PCOS) model through the anti-androgenic mechanism. Pharm Biol 2017;55(1):242–51.
[94] Unsal F, Sonmez MF. The effects of ovariectomy on ghrelin expression in the rat uterus. Adv Clin Exp Med 2014;23(3):363–70.
[95] Vanky E, Engen, Hanem LG, Abbott DH. Children born to women with polycystic ovary syndrome-short- and long-term impacts on health and development. FertiSteril 2019;111:1065–75.
[96] Cesta CE, Öberg AS, Ibrahimson A, Yusuf I, Larsson H, Almqvist C, D'Onofrio BM, et al. Maternal polycystic ovary syndrome and risk of neuropsychiatric disorders in offspring: prenatal androgen exposure or genetic confounding? Psychol Med 2019;12:1–9.
[97] Bracho GS, Altamirano GA, Kass L, Luque EH, Bosquiazzo VL. Hyperandrogenism induces histo-architectural changes in the rat uterus. Reprod Sci 2019;26(5): 657–68.
[98] Furat RS, Kurnaz OS, Eraldemır C, Sezer Z, Kum T, Ceylan S, et al. Effect of resveratrol and metformin on ovarian reserve and ultrastructure in PCOS: an experimental study. J Ovarian Res 2018;11:55.
[99] Adelakun SA, Ukweny VO, Akintunde OW. Vitamin B12 ameliorates Tramadol-induced oxidative stress, endocrine imbalance, apoptosis, and NO/iNOS/NF-κB expression in Sprague Dawley through a regulatory mechanism in the pituitary-gonadal axis. Tissue Cell 2021:101697.
[100] Alves ED, Bonfá ALO, Pigatto GR, Anselmo-Franci JA, Achcar JA, Parizotto NA, et al. Photobiomodulation can improve ovarian folliculogenesis and steroidogenesis in polycystic ovary syndrome-induced rats. Faseb J 2020;34.
[101] Adelakun SA, Ojewale AO, Jeje SO, Adedotun OA. Histomorphometric and biochemical activities of bioactive component of Cyprus esculentus extract on letrozole-induced polycysic ovarian syndrome and cholesterol homeostasis in female Sprague-Dawley rats. Toxicol Res Appl 2022;6:1–18.
[102] Zhang S, Tu H, Yao J, Le J, Jiang Z, Tang Q, et al. Combined use of diane-35 and metformin improves the ovulation in the PCOS rat model possibly *via* regulating glycolysis pathway. Reprod Biol Endocrinol 2020;18(1):58.